Collective motions of heterogeneous swarms

Klementyna Szwaykowska, Luis Mier-y-Teran Romero, and Ira B. Schwartz

U.S. Naval Research Laboratory
Code 6792
Plasma Physics Division
Nonlinear Dynamical Systems Section
Washington, DC 20375
klementyna.szwaykowska.ctr@nrl.navy.mil, lmieryt1@jhu.edu, ira.schwartz@nrl.navy.mil

Abstract— **The emerging collective motions of swarms of interacting agents are a subject of great interest in application areas ranging from biology to physics and robotics. In this paper, we conduct a careful analysis of the collective dynamics of a swarm of self-propelled heterogeneous, delay-coupled agents. We show the emergence of collective motion patterns and segregation of populations of agents with different dynamic properties; both of these behaviors (pattern formation and segregation) emerge naturally in our model, which is based on self-propulsion and attractive pairwise interactions between agents. We derive the bifurcation structure for emergence of different swarming behaviors in the mean field as a function of physical parameters and verify these results through simulation.**

NOTE TO PRACTITIONERS

Our research deals with understanding the emerging behaviors of groups of simple, interacting agents. The motivation for studying this subject is twofold: first, understanding the mechanisms that govern collective motions of biological organisms in processes like wound healing, cancer growth, flocking and herding, etc. Second, the application of our insights to synthesis of controllers for swarms of autonomous robotic agents to perform surveillance or monitoring in uncertain environments. Swarming behavior is typically modeled for groups of identical agents, under the assumption that sensing and processing times are negligibly small. We incorporate the real-world complications of (1) finite sensing/processing time, which appears as a delay in our model of agent motion, and (2) differences in the dynamical capabilities of swarming agents. We conduct a theoretical analysis of the collective motions of the swarm. We show the emergence of large-scale patterns in the swarm motion as a function of the physical parameters or the swarm, as well as segregation of the agents into separate groups where all agents in a given group have identical dynamics.

I. INTRODUCTION

The dynamics of aggregates, or swarms, of interacting mobile agents form an active area of study for biological, physical, and synthetic systems. Simple rules of interaction between agents can lead to a wide range of complex aggregate behaviors, even in the absence of leader agents and global motion strategy [1]. The emergence of rich collective

behaviors from simple interactions is, in fact, a wide-spread phenomenon in many application domains. In biology, the formation of aggregates is common on a wide range of spatio-temporal scales, for organisms ranging from bacteria to fish to birds and humans [2]–[6]. In robotics, aggregates of locally interacting agents have been proposed as a means to create scalable sensor arrays for surveillance and exploration [7], [8]; and for formation of reconfigurable modal systems, in which a group of simple agents can be used to accomplish a task that would be impossible for any agent individually, as in [9]–[11].

Understanding the dynamical characteristics of swarm behavior is essential for algorithm design and implementation. There is a wide range of existing works which model the dynamics of swarms on the level of individual agents [4]–[6], [12], as well as using continuum models [3], [13], [14]. It has been shown that, under the right conditions, swarms converge to organized steady-state behaviors; and furthermore, that environmental noise and/or processing delay acting on agent dynamics can lead to formation of new steady-state motions, or phase transitions between between co-existing steady states [1], [15], [16]. Noise is used to model effects of environmental disturbance and unknown interaction dynamics in robotic systems. Delays are important in biological modeling of population dynamics, blood cell production, and genetic networks [17]–[19], etc.; and in mathematical models of robot networks where communication and processing delays must be taken into account [20].

Most existing works assume that the swarm is made up of agents with identical dynamics. However, real-world swarms often include agents with varying dynamical properties, which leads to new collective behaviors. In biological systems, heterogeneity arises quite naturally when, for example, motion or sensing capabilities in an age-structured swarm vary significantly with age. A more striking example is that of of predator-prey interactions between a herd of prey animals and an individual or small group of predators, where there are distinct time-scale differences in the motion of predator and prey animals [6]. Another systems where heterogeneity plays a significant role is the segregation of intermingled cell types, as during growth and development of an organism. It has been shown that segregation can be

achieved simply by introducing heterogeneity in intercell adhesion properties [21], [22], or by increasing the intercell attraction between self-propelled cells of a single type [23].

An approach based on the cell segregation model in [23] is used in [24] to design a potential-based controller that achieves segregation in swarms of self-propelled autonomous robots. Heterogeneity also appears in robotic systems when individual robots with disparate capabilities are used together to achieve a common goal, as in [11]. Certain robots in the swarm may lack capabilities that are costly to implement. Stranieri *et al* [25], for example, show that flocking behavior can be achieved when a fraction of the agents lack the ability to align their velocities with those of their neighbors. Additionally, heterogeneity may arise over time as some agents in the swarm malfunction. For example, [26] introduces an observer to judge the overall "health" of a swarm, as individual agents lose speed from energy dissipation.

In this paper we carry out a systematic analysis of the motion of a swarm composed of heterogeneous agents, using the methodology outlined in [1]. We extend the model in [1] and analyze the dynamical behaviors of a heterogeneous swarm of delay-coupled agents, where the swarm is divided into two distinct populations with different motion capabilities. The inspiration for our model comes from the idea of using swarms of autonomous mobile agents as sensor platforms to survey/monitor an area of interest. Such agents may have different dynamical properties if, for example, some agents but not others are equipped with a particular sensor package that interferes with their motion. The package may be too expensive or otherwise impractical to mount on all swarm agents. Overall, allowing for heterogeneity in dynamical behaviors of swarm agents gives greater flexibility in system design, and is therefore desirable not only from a theoretical but also from a practical point of view.

The research presented here gives a general approach of modeling and analysis that can be used to understand the effects of individual agent dynamics on the collective motion of swarms. We know that swarms of self-propelled delay-coupled agents exhibit self-ordering and pattern formation, and that the collective patterns formed depend on the model parameters [1], [15]; furthermore, we observe in simulation that heterogeneity in the swarm composition leads to segregation of the individual swarm populations. We will show how collective motion patterns (translation, ring formation, and rotation about a common center of mass) and segregation of individual populations emerge in a basic but general swarming model.

II. PROBLEM STATEMENT

Consider a swarm of delay-coupled self-propelled agents, or robots, comprised of two distinct populations (1 and 2), following a single motion strategy, but with heterogeneous dynamics. The agents in Population 2 are less "maneuverable" in the sense that they are not able to accelerate as rapidly as those in Population 1. This setup models co-deployment of small, fast agents, and larger, slower agents in a given area. Let κ_1 and κ_2 be the inverse mass of agents

in Populations 1 and 2, respectively. We scale units so that $\kappa_1 = 1$ and $\kappa_2 = \kappa \in (0, 1)$.

Let $r_i^k \in \mathbb{R}^2$ denote the position of the ith agent in Population k ($k = 1, 2$); let N_1 and N_2 denote the number of agents in Populations 1 and 2, respectively; and let $N = N_1 + N_2$ be the total number of agents in the swarm. The agents have self-propulsion and are globally attracted to each other in a symmetric fashion, with coupling coefficient a, however, there is a delay τ in sensing of agent positions. For notational convenience, we introduce the following notation: let $\kappa_1 = 1$ and $\kappa_2 = \kappa$. The motion of the agents is governed by the following set of delay differential equations (dots denote differentiation with respect to time):

$$\ddot{r}_i^1 = \kappa_1 \left(1 - \left\| \dot{r}_i^1 \right\|\right)^2 \dot{r}_i^1 \tag{1a}$$
$$- \frac{a\kappa_1}{N} \left(\sum_{j \neq i, j=1}^{N_1} (r_i^1(t) - r_j^1(t-\tau)) \right. $$
$$\left. + \sum_{j=1}^{N_2} (r_i^1(t) - r_j^2(t-\tau)) \right)$$
$$\ddot{r}_i^2 = \kappa_2 \left(1 - \left\| \dot{r}_i^2 \right\|\right)^2 \dot{r}_i^2 \tag{1b}$$
$$- \frac{a\kappa_2}{N} \left(\sum_{j=1}^{N_1} (r_i^2(t) - r_j^1(t-\tau)) \right. $$
$$\left. + \sum_{j \neq i, j=1}^{N_2} (r_i^2(t) - r_j^2(t-\tau)) \right).$$

The first term in the above equations represents the self-propulsion of swarm agents, while the second models pairwise attraction between all agents in the swarm. This simplified model does not include short-range repulsion or other collision-avoidance strategies; however, earlier studies with homogeneous swarms indicate that the collective dynamics of the swarm are not significantly altered by the introduction of short-range repulsion terms.

The goal is now to characterize the steady-state motions of this system. Following the approach in [1], we begin by considering the dynamics in the limit where the number of agents goes to infinity.

III. MEAN-FIELD APPROXIMATION

Since basic collective swarm motions. as observed in simulation, consist of translation and rotation, the steady-state motions of the centers of mass of the individual populations are a means to characterize the motion of the overall group. Let R^1 and $R^2 \in \mathbb{R}^2$ denote the position of the centers of mass of Populations 1 and 2, respectively:

$$R^k(t) = \frac{1}{N_k} \sum_{i=1}^{N_k} r_i^k(t), \quad k = 1, 2. \tag{2}$$

As in [1], we assume that the deviations of the robots from the centers of mass of their respective populations are small. We analyze the steady-state motions of the swarm in the limit as $N_k \to \infty$ for $k = 1, 2$.

The positions of the agents in each population can be written relative to the respective center of mass as

$$r_i^k(t) = R^k(t) + \delta r_i^k(t). \tag{3}$$

Note that

$$\sum_{i=1}^{N_1} \delta r_i^1(t) = \sum_{i=1}^{N_2} \delta r_i^2(t) = 0. \tag{4}$$

For convenience, we introduce the notation

$$\bar{k} = \begin{cases} 2 & \text{for } k = 1 \\ 1 & \text{for } k = 2. \end{cases} \tag{5}$$

Substituting (3) into (1a) and simplifying the resulting expression using (4) allows us to write the equations of motion in terms of R^k and δr^k:

$$\ddot{R}^k + \delta \ddot{r}_i^k = \kappa_k \left(1 - \left\| \dot{R}^k + \delta \dot{r}_i^k \right\|^2 \right) \left(\dot{R}^k + \delta \dot{r}_i^k \right)$$
$$- \frac{a\kappa_k}{N} \Big((N_k - 1)(R^k(t) - R^k(t-\tau) \tag{6}$$
$$+ \delta r_i^k(t)) + \delta r_i^k(t-\tau)$$
$$+ N_{\bar{k}}(R^k(t) - R^{\bar{k}}(t-\tau) + \delta r_i^k(t)) \Big).$$

Summing the equations for δr_i^k over $i = 1, \ldots, N_k$, and dividing through by N_k, we get the equation of motion for the centers of mass of Population k:

$$\ddot{R}^k = \kappa_k \left(1 - \left\| \dot{R}^k(t) \right\|^2 \right) \dot{R}^k(t)$$
$$- \frac{\kappa_k}{N_k} \sum_{i=1}^{N_k} \Bigg(\left\| \delta \dot{r}_i^k \right\|^2 \dot{R}^k(t)$$
$$+ \left[\left\| \delta \dot{r}_i^k(t) \right\|^2 + 2\langle \dot{R}^k(t), \delta r_i^k(t) \rangle \right] \delta r_i^k(t) \Bigg) \tag{7}$$
$$- \frac{a\kappa_k}{N} \Big((N-1)R^k(t)$$
$$- (N_k - 1)R^k(t-\tau) - N_{\bar{k}}R^{\bar{k}}(t-\tau) \Big),$$

where $\langle \cdot, \cdot \rangle$ denotes the dot product in $\mathbb{R}^2$.

We now take the limit $N \to \infty$, while keeping the fraction of agents in Population 1,

$$c = N_1/N, \tag{8}$$

constant. Under the assumption of small deviations of the agents from the centers of mass of the respective populations, terms in δr_i^k can be neglected. We get the following equations for the motion of the center of mass of Population k ($k = 1, 2$):

$$\ddot{R}^k = \kappa_k \left(1 - \left\| \dot{R}^k(t) \right\|^2 \right) \dot{R}^k(t)$$
$$- a\kappa_k \Big(R^k(t) - cR^1(t-\tau) - (1-c)R^2(t-\tau) \Big). \tag{9}$$

Let $[X_k, Y_k] = R^k$ and $[U_k, V_k] = \dot{R}^k$ denote, respectively, the position and velocity of the center of mass of population $k = 1, 2$. Let superscript τ denote a delay τ, so that $X^\tau(t) =$

$X(t-\tau)$. The equations of motion can be written in terms of X_k, Y_k, U_k, and V_k as

$$\dot{X}_k = U_k \tag{10a}$$
$$\dot{Y}_k = V_k \tag{10b}$$
$$\dot{U}_k = \kappa_k(1 - U_k^2 - V_k^2)U_k$$
$$- a\kappa_k(X_k - cX_1^\tau - (1-c)X_2^\tau) \tag{10c}$$
$$\dot{V}_k = \kappa_k(1 - U_k^2 - V_k^2)V_k$$
$$- a\kappa_k(Y_k - cY_1^\tau - (1-c)Y_2^\tau). \tag{10d}$$

The system in (10) has an invariant stationary solution given by

$$\begin{aligned} X_1 = X_2 = X_0, &\qquad Y_1 = Y_2 = Y_0 \\ U_1 = U_2 = 0, &\qquad V_1 = V_2 = 0, \end{aligned} \tag{11}$$

as well as a translating solution where the center of mass travels in a straight line at constant velocity.

A. Bifurcation of the stationary solution

About the stationary solution, the system exhibits a number of Hopf bifurcations for different values of the parameters a, c, κ, and τ. To find the locations of these bifurcation points, consider the linearization of the dynamics (10) about the stationary solution (without loss of generality, we choose $X_0 = Y_0 = 0$). The linearized dynamics are

$$\dot{X}_k = U_k \tag{12a}$$
$$\dot{Y}_k = V_k \tag{12b}$$
$$\dot{U}_k = \kappa_k U_k - a\kappa_k \Big(X_k - cX_1^\tau - (1-c)X_2^\tau \Big) \tag{12c}$$
$$\dot{V}_k = \kappa_k V_k - a\kappa_k \Big(Y_k - cY_1^\tau - (1-c)Y_2^\tau \Big). \tag{12d}$$

Let $\xi = [X_1, Y_1, U_1, V_1, X_2, Y_2, U_2, V_2]^T$. The above system takes the form $\dot{\xi} = \mathcal{L}\xi$, where $\mathcal{L}$ is a linear operator. Let ν denote an eigenvector of $\mathcal{L}$; then a solution starting at ν can be expressed as $e^{\lambda t}\nu$. This equation can only be satisfied if the matrix $M(\lambda; a, c, \kappa, \tau)$ is singular, where $M = \lambda I - \mathcal{L}$. That is, λ must satisfy $0 = \det M = D^2$, where

$$D(\lambda; a, c, \kappa, \tau) = (\lambda^2 - \lambda + a)(\lambda^2 - \kappa\lambda + a\kappa)$$
$$- ((\kappa + c - \kappa c)\lambda^2 - \kappa\lambda + a\kappa)ae^{-\lambda\tau}. \tag{13}$$

Hopf bifurcations of the mean-field equations occur when $\text{Re}(\lambda) = 0$. Setting $\lambda = i\omega$ gives $D(i\omega; a, c, \kappa, \tau) = 0$ which allows us to solve for parameter values of where Hopf bifurcations occur. Solutions in terms of a and τ, for different values of c and κ, are shown by the solid blue lines in Fig. 1.

Below the first Hopf bifurcation curve, the mean-field predicts a stationary state which corresponds to a ring state in the full swarm dynamics. This is similar to the ring state described in [1], where swarm agents circle about a stationary center of mass in either direction, with constant radius and speed. The first Hopf bifurcation in the mean-field approximation gives rise to a rotating state analogous to the one in [1], in which the centers of mass of the swarm
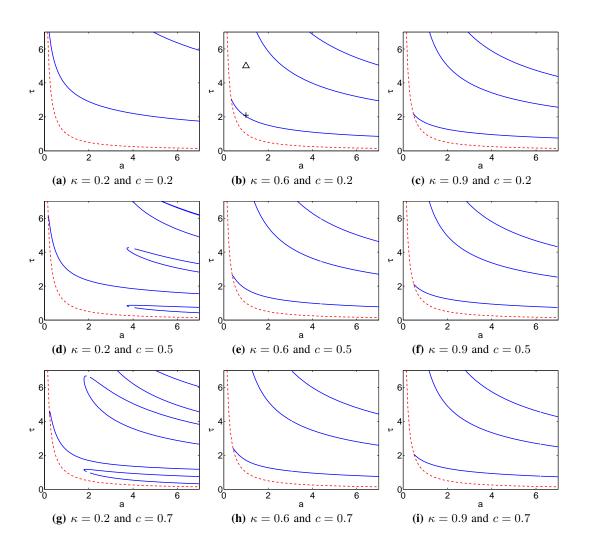
(a) $\kappa = 0.2$ and $c = 0.2$ **(b)** $\kappa = 0.6$ and $c = 0.2$ **(c)** $\kappa = 0.9$ and $c = 0.2$

(d) $\kappa = 0.2$ and $c = 0.5$ **(e)** $\kappa = 0.6$ and $c = 0.5$ **(f)** $\kappa = 0.9$ and $c = 0.5$

(g) $\kappa = 0.2$ and $c = 0.7$ **(h)** $\kappa = 0.6$ and $c = 0.7$ **(i)** $\kappa = 0.9$ and $c = 0.7$

Fig. 1: The solid blue lines show τ vs a Hopf bifurcation curves for the center-of-mass heterogeneous swarm dynamics, for different values of the parameters c and κ. The location of the pitchfork bifurcation where the translating state disappears is shown by the dashed red curve. The point where the Hopf curve intersects the pitchfork bifurcation curve is the Bogdanov-Takens point. The "Δ" and "+" in **(b)** show the points in parameter space corresponding to the simulations in Fig. 2 and Fig. 4, respectively.

populations rotate about a common stationary point. Higher-order Hopf bifurcations lead to formation of rotating states with higher angular frequency, but these states appear to be unstable, based on our simulations with homogeneous swarms. The introduction of heterogeneity leads to a separation between the agents in the two populations in both of these steady state motions.

B. Ring State

The ring state in the heterogeneous swarm is similar to that described in [1] for homogeneous agent swarms; that is, agents move in either direction about a stationary center of mass, with constant speed and radius. The heterogeneity introduces a split in the rings formed by the agents of the two populations, however, so that they become separated (see Fig. 2).

It can be shown that the angular frequency ω_i and radius

ρ_i of the particles in population $i = 1, 2$ satisfy

$$\rho_1 = 1/\sqrt{a} \quad \omega_1 = \sqrt{a} \tag{14}$$
$$\rho_2 = 1/\sqrt{a\kappa} \quad \omega_2 = \sqrt{a\kappa} \tag{15}$$

(see Appendix for details). Note that the radius for each population depends only on the strength of the coupling constant and the acceleration factor; that is, the radii of the two populations are not coupled and are independent of the time delay τ.

The above calculations were verified using a full-swarm simulation with 300 agents, and different values of the parameters a, κ, c, and τ. The results of comparing the ring radii and angular velocities obtained from simulation and theory are shown in Fig. 3.

C. Rotating State

The rotating state, like the ring state, is also present in the case of a homogeneous swarm [1]. In the rotating state,
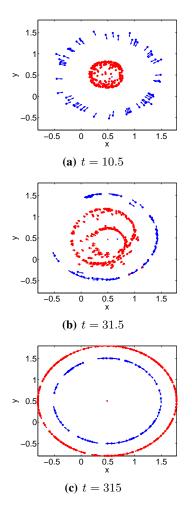
(a) $t = 10.5$

(b) $t = 31.5$

(c) $t = 315$

Fig. 2: Simulated swarm of $N = 300$ agents, with 60 agents in Population 1 (blue) and 240 in Population 2 (red), converging to the ring state. In this simulation, $\kappa = 0.6$, $c = 0.2$, $a = 1.0$, and $\tau = 2.1$. This point in parameter space is marked by a "Δ" in Fig. 1b.

the swarm populations collapse to their respective centers of mass and rotate about a common center point with constant phase offset (see Fig. 4).

Our numerical simulations of the full swarm dynamics suggest that the radii of the rotating populations are equal. Let ρ denote the radius of the rotating state, ω the angular frequency, and let $\Delta\theta = \theta_2 - \theta_1$ denote the phase offset. It can be shown (see Appendix for details) that these quantities must satisfy the following relations:

$$\sin \Delta\theta = (2c - 1)P(c, \kappa, \omega) \sin \omega\tau \quad (16)$$

$$\omega^2 = a\kappa\Big[1 - \cos \omega\tau \quad (17)$$

$$+ c((2c - 1)\sin^2 \omega\tau + \cos^2 \omega\tau)P(c, \kappa, \omega)\Big] \quad (18)$$

$$\rho = \frac{\sqrt{1 - a\left(1 - 2c(1 - c)P(c, \kappa, \omega)\cos \omega\tau\right)\frac{\sin \omega\tau}{\omega}}}{|\omega|}. \quad (19)$$
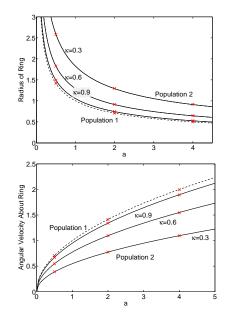

Fig. 3: Comparison of theoretical and simulated radius and angular velocity in the ring state. Theoretical values are shown by the solid lines, while values obtained from simulations are shown by the red crosses. The simulations were run for a swarm of $N = 300$ agents, with fraction in Population 1 $c = 0.2$ and time delay $\tau = 1.0$.
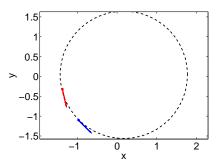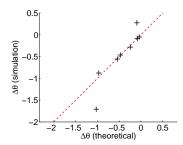

Fig. 4: Swarm in the rotating state at $t = 323.8$. Agents in Population 1 are shown in blue, while those in Population 2 are in red. The dotted circle shows the trajectory of the two swarm populations about a common stationary point. The simulation was run with $N = 300$ agents, with $N_1 = 60$ and $N_2 = 240$. The parameter values are: $\kappa = 0.6$, $c = 0.2$, $a = 1.0$, and $\tau = 5.0$. This point in parameter space is marked by a "+" in Fig. 1b.
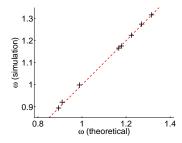
where

$$P(c, \kappa) = \frac{(1 - \kappa)(1 - \cos \omega\tau)}{(1 + k)c - 1 + 2(1 - \kappa)c(1 - c)\sin^2 \omega\tau}. \quad (20)$$
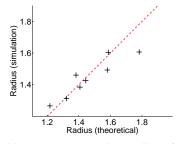
The above relations may be used to derive theoretical values for the radius, angular velocity, and phase offset between Populations 1 and 2. A comparison of the theoretical values and those observed in full-swarm simulations is shown in Fig. 5, for different values of the parameters κ, c, a, and τ. Note that the above relations, derived from the mean-field approximation, give a good approximation to values obtained from the full swarm simulation; however, in some cases, the

use of the mean-field approximation leads to significant error in computed values.

(a) Real vs. theoretical phase difference between the two swarm populations.

(b) Real vs. theoretical angular frequency for the rotating state.

(c) Real vs. theoretical radius of the rotating state.

Fig. 5: Comparison of theoretical and simulated phase difference, angular velocity, and radius in the rotating state. Theoretical values are along the x-axis, while values obtained from simulations are along the y-axis. The simulations were run for a swarm of 300 agents, for $\kappa = 0.3, 0.6, 0.9$, $c = 0.2$, $a = 0.5, 1.0, 2.0, 4.0$, and $\tau = 4.0, 5.0$.

D. Translating state

The system in (10) has a steady-state translating solution, where $\dot{U}_1 = \dot{U}_2 = \dot{V}_1 = \dot{V}_2 = 0$, $U_1 = U_2 = U_0$, $V_1 = V_2 = V_0$, and

$$X_1(t) = X_2(t) = X_0 + U_0 t \qquad (21a)$$
$$Y_1(t) = Y_2(t) = Y_0 + V_0 t. \qquad (21b)$$

U_0 and V_0 must satisfy:

$$U_0^2 + V_0^2 = 1 - a\tau, \qquad (22)$$

which is possible only if $a\tau \leq 1$. In fact, the system (10) has a pitchfork bifurcation along the parameter-space curve
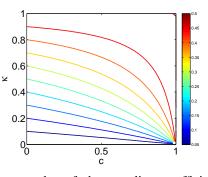

Fig. 6: Contour plot of the coupling coefficient at the Bogdanov-Takens point a_{BT} as a function of κ and c. Different values of a_{BT} are shown by the colors (see colorbar on the right).

$\tau = 1/a$ (see Fig. 1), where the stationary solution gives rise to the translating state (the other branch of the pitchfork corresponds to an unphysical solution with imaginary speed). The same bifurcation curve exists in the homogeneous system ($\kappa = 1$) [1].

The point where the pitchfork bifurcation coincides with the first Hopf curve is a Bogdanov-Takens (BT) point (see Fig. 1). In the homogeneous swarm case, this point is located at $a = 1/2$, $\tau = 2$; for the heterogeneous swarm the location of the point depends on the acceleration factor κ and on the fraction c of agents in Population 1. The BT point is at

$$a_{BT} = \frac{\kappa}{2(1 - c(1 - \kappa))} \qquad (23)$$
$$\tau_{BT} = \frac{1}{a_{BT}}. \qquad (24)$$

The value of coupling coefficient at the Bogdanov-Takens point a_{BT} as a function of κ and c is shown in Fig. 6.

IV. Conclusion

In this paper we have analyzed the collective motions of a swarm of delay-coupled heterogeneous agents. The swarm motions are characterized by the emergence of large-scale patterns (translation, ring formation, and rotation), and the automatic segregation of populations of agents with different dynamical properties. Separation of the swarm into distinct populations is a direct consequence of swarm heterogeneity, and is not observed under homogeneous swarm dynamics.

The patterns observed in simulation were shown to arise in the motions of the swarm center of mass, in the limit as the number of agents in each population goes to infinity. We derive expressions for the speed of the swarm in the translating state as a function of time delay and coupling coefficient; for the radii and angular velocities of both agent populations in the ring and rotating states; and for the fixed phase offset between populations in the rotating state. We have verified these calculations with simulations of the full-swarm dynamics. In spite of discrepancies, it is remarkable that our model reduction, which starts with N second-order delay-differential equations and yields one equation of the same type, is able to quantitatively capture so many aspects of the full swarm dynamics.

A real-world model of swarming physical agents must incorporate a collision-avoidance strategy. This could be implemented, for example, by adding a short-range repulsion to the agent dynamics. Such interactions may affect the collective motion of the swarm to some degree, but our preliminary simulations of homogeneous swarms indicates that the qualitative behavior of the swarm is not affected by short-range repulsion forces. This will be addressed more carefully in a future paper.

In our model, we have assumed that the motion of each agent in the swarm depends on the positions of all other agents. In future work, we will relax this assumption to model the effects of non-global coupling on the collective swarm motion; we will also add noise to the swarm dynamics. We know that adding noise causes switching between co-existing stable states (ring and rotating state) in homogeneous swarms [1]. We will investigate how switching behavior changes when the swarm is made up of heterogeneous agents.

Our work presents new insights into the collective motions of aggregates of heterogenous, self-propelled agents, whether biological or artificial. Our results are important from a practical design standpoint for artificial systems, as when a swarm of robots is used to survey/monitor a given area of interest. In addition to their relevance in the study of swarming and herding motions in biological systems, our results on heterogeneity play a predictive role where the dynamics of individual agents are to large degree beyond our control.

ACKNOWLEDGMENTS

APPENDIX
RING STATE

In the ring state, the agents in either population rotate about a common stationary center of mass. To study the dynamics of the ring state, we must therefore re-introduce the full swarm dynamics. For convenience, we express these in polar coordinates, with the origin located at the position of the stationary center of mass, so that $R^1(t) = R^2(t) \equiv 0$. Then let

$$\rho_i^1 k = \left\| \delta r_i^k \right\|, \quad \theta_i^k = \angle \delta r_i^k \quad (25)$$

for $k = 1, 2$. Setting $R^k = \dot{R}^k = \ddot{R}^k = 0$ in (6) gives:

$$\delta \ddot{r}_i^k = \frac{\kappa_k}{N_k} \sum_{j=1}^{N_k} \left\| \delta \dot{r}_j^k \right\|^2 \delta \dot{r}_j^k + \kappa_k \left(1 - \left\| \delta \dot{r}_i^k \right\|^2 \right) \delta \dot{r}_i^k \\ - \frac{a \kappa_k}{N} \left((N-1)\delta r_i^k + \delta r_i^{k,\tau} \right). \quad (26)$$

In the ring state, $R^k = \dot{R}^k = \ddot{R}^k = 0$ requires that $\sum_{j=1}^{N_k} \left\| \delta \dot{r}_j^k \right\|^2 \delta \dot{r}_j^k = 0$ for $k = 1, 2$ [1]; so that, in the

limit as $N \to \infty$,

$$\delta \ddot{r}_i^k = \kappa_k \left(1 - \left\| \delta \dot{r}_i^k \right\|^2 \right) \delta \dot{r}_i^k - a \kappa_k \delta r_i^k. \quad (27)$$

Converting to polar coordinates leads to the following set of equations:

$$\ddot{\rho}_i^k = \kappa_k \dot{\rho}_i^k \left(1 - (\rho_i^k \dot{\theta}_i^k)^2 - (\dot{\rho}_i^k)^2 \right) + \left((\dot{\theta}_i^k)^2 - a \right) \rho_i^k \quad (28a)$$

$$\rho_i^k \ddot{\theta}_i^k = \kappa_k \rho_i^k \dot{\theta}_i^k \left(1 - (\rho_i^k \dot{\theta}_i^k)^2 - (\dot{\rho}_i^k)^2 \right) - 2\dot{\rho}_i^k \dot{\theta}_i^k. \quad (28b)$$

Note that the equations governing the two populations are entirely uncoupled. In the ring state, $\dot{\rho}_i^k = \ddot{\rho}_i^k = 0$ and the agents move with constant angular velocity so that $\ddot{\theta}_i^k = 0$ for $k = 1, 2$. Let ω_i^k denote the constant angular velocity $\dot{\theta}_i^k$ of agent i in population k. Then (28) can be written as:

$$0 = \left((\omega_i^k)^2 - a\kappa_k \right) \rho_i^k \quad (29a)$$
$$0 = \rho_i^k \omega_i^k \left(1 - (\rho_i^k \omega_i^k)^2 \right), \quad (29b)$$

and it follows that

$$\rho_i^k = 1/|\omega_i^k|, \quad \omega_i^k = \pm\sqrt{a\kappa_k} \quad (30)$$

for all agents in the swarm.

APPENDIX
ROTATING STATE

To find the parameters describing the rotating state of the swarm, we convert the equations for the swarm dynamics to polar coordinates. Suppose that the ring state is formed about the stationary point $(X_s, Y_s)^T \in \mathbb{R}^2$, and choose the origin of the polar coordinates to lie on $(X_s, Y_s)^T$. Let (ρ_k, θ_k) denote the position, in polar coordinates, of the center of mass of Population k, that is

$$\rho_k = \sqrt{(X_k - X_s)^2 + (Y_k - Y_s)^2} \quad (31a)$$

$$\theta_k = \tan^{-1} \frac{Y_k - Y_s}{X_k - X_s}. \quad (31b)$$

The equations of motions for the motion of the centers of mass of the two swarm populations in polar coordinates, are

$$\ddot{\rho}_k = \kappa_k \left(1 - \rho_k^2 \dot{\theta}_k^2 - \dot{\rho}_k^2 \right) \dot{\rho}_k + \rho_k \dot{\theta}_k^2 \\ - a\kappa_k \left(\rho_k - c\rho_1^\tau \cos(\theta_k - \theta_1^\tau) \right. \quad (32a) \\ \left. - (1-c)\rho_2^\tau \cos(\theta_k - \theta_2^\tau) \right)$$

$$\rho_k \ddot{\theta}_k = \kappa_k \left(1 - \rho_k^2 \dot{\theta}_k^2 - \dot{\rho}_k^2 \right) \rho_k \dot{\theta}_k - 2\dot{\rho}_k \dot{\theta}_k \\ - a\kappa_k \left(c\rho_1^\tau \sin(\theta_k - \theta_1^\tau) \right. \quad (32b) \\ \left. + (1-c)\rho_2^\tau \sin(\theta_k - \theta_2^\tau) \right).$$

In the rotating state, the radii of the populations and the angular frequencies are constant. Let $\omega_k = \dot{\theta}_k$. Then

$$\rho_k(t) = \rho_k^0 \quad (33a)$$
$$\theta_k(t) = \theta_k^0 + \omega_k t, \quad (33b)$$

and $\ddot{\rho}_k = \dot{\rho}_k = \ddot{\theta}_k = 0$. Furthermore, simulations of the full swarm dynamics suggest that the radii of the two populations

in the rotating state are equal; we therefore set $\rho_1^0 = \rho_2^0 = \rho$. Let $\Delta\theta = \theta_1 - \theta_2$ denote the phase difference between the two populations. Substituting these equations into (32) and simplifying the resulting expressions gives:

$$
\begin{aligned}
\omega_k^2 = a\kappa_k\big(1 &- c\cos(\omega_1\tau + (\omega_k - \omega_1)t + \theta_k^0 - \theta_1^0) \\
&- (1-c)\cos(\omega_2\tau + (\omega_k - \omega_2)t + \theta_k^0 - \theta_2^0)\big)
\end{aligned}
\tag{34a}
$$

$$
\begin{aligned}
(1 - \rho^2\omega_k^2)\omega_k = a\kappa_k\big(&c\sin(\omega_1\tau + (\omega_k - \omega_1)t + \theta_k^0 - \theta_1^0) \\
&+ (1-c)\sin(\omega_2\tau + (\omega_k - \omega_2)t + \theta_k^0 - \theta_2^0)\big).
\end{aligned}
\tag{34b}
$$

Note that the time dependence on the right hand sides of all equations in (34) can be eliminated if and only if $\omega_1 = \omega_2$. Let ω denote the common frequency of both populations about the center. Thus, we finally have the four equations describing the behavior of the swarm in the ring state:

$$
\begin{aligned}
\omega^2 = a\kappa_k\big(1 &- c\cos(\omega\tau + \theta_k^0 - \theta_1^0) \\
&- (1-c)\cos(\omega\tau + \theta_k^0 - \theta_2^0)\big)
\end{aligned}
\tag{35a}
$$

$$
\begin{aligned}
(1 - \rho^2\omega^2)\omega = a\kappa_k\big(&c\sin(\omega\tau + \theta_k^0 - \theta_1^0) \\
&+ (1-c)\sin(\omega\tau + \theta_k^0 - \theta_2^0)\big).
\end{aligned}
\tag{35b}
$$

Relations (16)-(19) can be derived from (35) through some rather involved algebraic manipulations.

REFERENCES

[1] L. Mier-y-Teran Romero, E. Forgoston, and I. B. Schwartz, "Coherent Pattern Prediction in Swarms of Delay-Coupled Agents," IEEE Transactions on Robotics, vol. 28, pp. 1034–1044, Oct. 2012.

[2] E. O. Budrene and H. C. Berg, "Dynamics of formation of symmetrical patterns by chemotactic bacteria," Nature, vol. 376, pp. 49–53, 1995.

[3] A. A. Polezhaev, R. A. Pashkov, A. I. Lobanov, and I. B. Petrov, "Spatial patterns formed by chemotactic bacteria Escherichia coli," The International journal of developmental biology, vol. 50, pp. 309–314, Jan. 2006.

[4] K. r. Tunstrø m, Y. Katz, C. C. Ioannou, C. Huepe, M. J. Lutz, and I. D. Couzin, "Collective states, multistability and transitional behavior in schooling fish," PLoS computational biology, vol. 9, p. e1002915, Jan. 2013.

[5] D. Helbing and P. Molnar, "Social force model for pedestrian dynamics," Physical Review E, vol. 51, no. 5, pp. 4282–4286, 1995.

[6] S.-H. Lee, "Predator's attack-induced phase-like transition in prey flock," Physics Letters A, vol. 357, pp. 270–274, Sept. 2006.

[7] P. Bhatta, E. Fiorelli, F. Lekien, N. E. Leonard, D. A. Paley, F. Zhang, R. Bachmayer, D. M. Fratantoni, R. E. Davis, and R. J. Sepulchre, "Coordination of an underwater glider fleet for adaptive sampling," in Proceedings of the International Workshop on Underwater Robotics, no. August, pp. 61–69, 2005.

[8] W. Wu and F. Zhang, "Cooperative exploration of level surfaces of three dimensional scalar fields," Automatica, vol. 47, pp. 2044–2051, Sept. 2011.

[9] K. M. Lynch, I. B. Schwartz, P. Yang, and R. A. Freeman, "Decentralized Environmental Modeling by Mobile Sensor Networks," IEEE Transactions on Robotics, vol. 24, pp. 710–724, June 2008.

[10] S. Kar and J. M. F. Moura, "Distributed linear parameter estimation in sensor networks: Convergence properties," Oct. 2008.

[11] M. Dorigo, D. Floreano, L. M. Gambardella, F. Mondada, S. Nolfi, T. Baaboura, M. Birattari, M. Bonani, M. Brambilla, A. Brutschy, D. Burnier, A. Campo, A. L. Christensen, A. Decugniere, G. Di Caro, F. Ducatelle, E. Ferrante, A. Forster, J. M. Gonzales, J. Guzzi, V. Longchamp, S. Magnenat, N. Mathews, M. Montes de Oca, R. O'Grady, C. Pinciroli, G. Pini, P. Retornaz, J. Roberts, V. Sperati, T. Stirling, A. Stranieri, T. Stutzle, V. Trianni, E. Tuci, A. E. Turgut, and F. Vaussard, "Swarmanoid: A Novel Concept for the Study of Heterogeneous Robotic Swarms," IEEE Robotics & Automation Magazine, vol. 20, pp. 60–71, Dec. 2013.

[12] T. Vicsek, A. Czirok, E. Ben-Jacob, I. Cohen, and O. Shochet, "Novel type of phase transition in a system of self-driven particles," 2006.

[13] L. Edelstein-Keshet, D. Grunbaum, and J. Watmough, "Do travelling band solutions describe cohesive swarms? An investigation for migratory locusts," Journal of Mathematical Biology, vol. 36, pp. 515–549, July 1998.

[14] C. M. Topaz and A. L. Bertozzi, "Swarming Patterns in a Two-Dimensional Kinematic Model for Biological Groups," SIAM Journal on Applied Mathematics, vol. 65, pp. 152–174, Jan. 2004.

[15] L. Mier-y-Teran Romero, E. Forgoston, and I. B. Schwartz, "Noise, Bifurcations, and Modeling of Interacting Particle Systems," in Proceedings of the IEEE/RSJ International Conference on Intelligent Robots and Systems, pp. 3905–3910, Jan. 2011.

[16] B. S. Lindley, L. Mier-y-Teran Romero, and I. B. Schwartz, "Noise Induced Pattern Switching in Randomly Distributed Delayed Swarms," in Proc. 2013 American Control Conference (ACC 2013), pp. 4587–4591, 2013.

[17] A. Martin and S. Ruan, "Predator-prey models with delay and prey harvesting," Journal of Mathematical Biology, vol. 43, pp. 247–267, Sept. 2001.

[18] S. Bernard, J. Bélair, and M. C. Mackey, "Bifurcations in a white-blood-cell production model," Comptes Rendus Biologies, vol. 327, pp. 201–210, Mar. 2004.

[19] N. A. M. Monk, "Oscillatory Expression of Hes1, p53, and NF-kB Driven by Transcriptional Time Delays," Current Biology, vol. 13, pp. 1409–1413, 2003.

[20] E. Forgoston and I. B. Schwartz, "Delay-induced instabilities in self-propelling swarms," Physical Review E, vol. 77, no. 302, p. 035203, 2008.

[21] M. S. Steinberg, "Reconstruction of Tissues by Dissociated Cells," Science, vol. 141, pp. 401–408, Aug. 1963.

[22] F. Graner, "Simulation of the differential adhesion driven rearrangement of biological cells," Physical Review E, vol. 47, no. 3, pp. 2128–2154, 1993.

[23] J. Belmonte, G. Thomas, L. Brunnet, R. de Almeida, and H. Chaté, "Self-Propelled Particle Model for Cell-Sorting Phenomena," Physical Review Letters, vol. 100, p. 248702, June 2008.

[24] M. Kumar, D. P. Garg, and V. Kumar, "Segregation of Heterogeneous Units in a Swarm of Robotic Agents," IEEE Transactions on Automatic Control, vol. 55, no. 3, pp. 743–748, 2010.

[25] A. Stranieri, E. Ferrante, A. E. Turgut, V. Trianni, C. Pinciroli, M. Birattari, and M. Dorigo, "Self-Organized Flocking with a Heterogeneous Mobile Robot Swarm," in Advances in Artificial Life, ECAL 2011: 11th European Conference on the Synthesis and Simulation of Living Systems, no. 2002, pp. 789–796, 2010.

[26] P. M. Kingston, M. Egerstedt, and E. I. Verriest, "Health monitoring of networked systems," in Mathematical Theory of Networked Systems (MTNS), 2008.